EXPERIMENTAL STUDY OF PHOTOTHERMAL CONVERSION OF HEAT ABSORBERS FILLED WITH METAL FOAMS OF DIFFERENT PORE DENSITIES

*Junhu HU[a,b], Kaiqiang HU[a,b], Lei XIN[a,b], Hao LIU[c], Xiaohong YANG[a,b], Shunli WU[d,e]**

[a]College of Energy and Power Engineering, Inner Mongolia University of Technology, Hohhot, P.R. China

[b]Inner Mongolia Key Laboratory for Renewable Energy, Hohhot, P.R. China

[c]Hohhot Thermal Power Plant, Hohhot, P.R. China

[d]College of Marine Life Sciences, Ocean University of China

[e]Hangzhou Singclean Medical Products CO, LTD

[*]Corresponding author; E-mail: shunliwu@shu.edu.cn

High output temperature and photothermal conversion effectiveness were achieved with the absorber platform structure. A novel solar receiver was manufactured to integrate pre-heating and thermal conversion, aiming to enhance heat utilization and output temperature. This work is based on the engineering design and experimental testing of a solar cavity-receiver containing a porous copper foam that can volumetrically absorb high-flux radiation and heat up, through convection with air flow. The air outlet temperature, outer wall temperature, thermal performance, and efficiency were experimentally determined by pore density, air mass flow rate and solar irradiance. Additionally, the temperature growth of unit incident power (ζ), the unit volume efficiency growth rate (ψ) and output temperature were employed to evaluate the thermal conversion characteristics of the endothermic body (copper foam). The results indicated that the air outlet temperatures can reach 500 ℃ with lower input power. Furthermore, it was found that under a pore density of 30 pores per inch and a flow rate of 60 $L \cdot min^{-1}$, the photothermal conversion efficiency of the absorber with copper foam reached as high as 87.61%, which is 35.04% significantly higher than that of an absorber without copper foam. The manageable solar receiver design proved to deliver a high-temperature air flow (approximately 500 ℃) with a reasonably high thermal efficiency (over 85%).

Key words: metal foam, photothermal conversion, absorber, pore density

1. Introduction

Currently, the global concern over energy shortage has heightened due to the escalating greenhouse gas emissions and the depletion of fossil resources. To mitigate these pressing global issues, there is an urgent need to explore and exploit renewable energy resources (such as wind [1], solar [2], tidal, nuclear [3] and etc.). Due to its universality, harmlessness, and abundant availability, solar energy holds excellent promise for the renewable energy system [4]. Moreover, the concept of

distributed solar energy (photothermal conversion) [5-7] has emerged as a new approach to offer significant support for the future trajectory of renewable energy development according to the regional climate characteristics. However, the efficiency of photothermal conversion is limited by the heat absorber's efficiency. Therefore, the development of heat transfer absorbers that enhance thermal efficiency has become a critical strategy to facilitate energy conversion efficiency.

To address above problem, various strategies are exploited to optimize the performance of absorbers (e.g., metamaterial absorber [8], metamaterial perfect absorber (MPA) [9], porous material [10], etc.). Metal foams (MFs), with characteristics such as high strength, high porosity, excellent insulation properties, and large specific surface area, are considered ideal candidates for improving energy efficiency in current research. MFs were found widespread applications in various fields, such as manufacturing, environmental protection, aerospace, petrochemicals, especially in filtration and environmental protection domains. The thermal utilization performance of solar collectors can be tremendously improved by enhancing the absorbed heat via applying MFs [11]. Moreover, the experimental studies have shown that the Parabolic Trough Collector (PTC) performance of a porous plate solar trough collector with Alternative Porous Disc Receiver (APDR) is superior to other receiver configurations [12]. Compared with traditional tubular receivers, the thermal gradient between the receiver wall and the fluid, as well as between the receiver cross-section, is reduced in the porous disk-enhanced receiver. This is advantageous for improving the heat collection performance of trough collectors. However, the dish solar concentrator is widely used in the medium to high-temperature collection process due to its strong focusing and heat collection characteristics. Dong X. H. [13] developed an efficient and compact structural technology scheme and built a solar thermal conversion experimental platform combined with a newly designed photothermal conversion device. The high-temperature heat conversion process in the absorber was numerically simulated using Fluent software, and the experimental results demonstrated that the photothermal conversion efficiency of the absorber can reach up to 88.63%. Based on the absorber's characteristics, a novel type of Zirconium Diboride (ZrB_2) foam absorber [14] was developed and compared against a silicon carbide (SiC) honeycomb absorber, revealing MFs with small pore size and low porosity had higher thermal absorption efficiency. Furthermore, to solve the issue of unequal energy flow distribution within the cavity-type absorber in the conventional Stirling power generation system [15], Meng et al. [16] adopted a light propagation approach, which led to the development and comparison of novel free-form reflection mirror surfaces and triangular cavity receivers [17], both of which could effectively alleviate this problem. This solar volumetric receiver is designed to lay the groundwork for industrial application of high-temperature heat utilization around the clock. In heat transfer and energy storage applications, Yu C. L. [18] used Monte Carlo method to simulate the thermal radiation characteristics of a two-dimensional porous medium and analyzed the effect of inlet flow rate on the radiative heat loss. Jiang Z. W. [19] carried out an experimental study on the designed foam metal heat absorber, and after measurements, it was concluded that the outlet temperature of the absorber was 463 °C and the thermal efficiency of the experimental system reached 81.5%. Xu C. et al. [20] chose the optimal volume convection heat transfer coefficient model and applied the steady state heat transfer model of porous media to the porous media tower receiver, combined with the porosity of the material, particle diameter, etc., the analysis yielded that the temperature of the solid matrix of the porous media with a porosity of 0.15 is 1585 K, which is 250 K higher than that of the porous material with a porosity of 0.35. And a porous medium with a large particle size (0.125 mm) was used

to the receiver. The temperature is reaches the highest up to 1762 K at the receiving surface. In comparison, Wang Y. Q. [21] simulated the heat transfer of a bilayer SiC absorber with different structural parameters using COMSOL MUTIPHSICS software. It was concluded that the highest simulated temperature of 1712 K can be reached at the outlet of the material with a thickness ratio of 0.2 and its porosity increased from 0.6 to 0.8. To further investigate the heat transfer enhancement capabilities of MF, Dixit and Ghosh [22] have conducted experiments that involve placing copper foam between inter-layer plates under constant temperature conditions and have studied the relevant data to improve the heat transfer performance of MF on the surface in question. Cao Y. [23] et al. designed an absorber structure utilizing porous copper foam, rotating and nanofluid materials, which increased the heat collection performance of the collector from 77.6% to 88.1%. Similarly, this performance increase can be achieved by controlling the flow rate and inlet temperature [10]. Specifically, the area benign coefficient of the MF material used for heat absorber is superior to that of finned heat exchanger.Yang B. [24] et al. conducted energy storage experiments with three composites, “nanoparticle/paraffin”, “metal foam/paraffin” and “nanoparticle/metal foam/paraffin”, respectively, in place of the pure paraffin phase change material. The thermal storage performance was enhanced to 123.27%, 740.39% and 847.15% of the original, respectively; meanwhile, the melting time and solidification time of the phase change materials were shortened. On this basis, Wang Z. L. [25] et al. experimented by mixing copper metal foam with paraffin wax in different ratios, which resulted in an increase in the heat storage rate and the integrated heat transfer coefficient from 21.81 J/s to 25.08 J/s, and 1.26 $W \cdot m^{-1} \cdot K^{-1}$ to 4.16 $W \cdot m^{-1} \cdot K^{-1}$, respectively. It was also found that the heat transfer mechanism was dominated by natural convection in the lower percentage of composites, while heat conduction played a major role in the higher percentage.Tian Y. [26] et al. focused on the effect of metal foam on the enhancement of heat transfer in phase change materials (PCMs), and it was measured that both metal foams with smaller porosity and larger pore density could further increase the heat transfer rate. Combining MF with one or more phase change materials has been shown to further enhance the heat transfer performance of the receiver, which is important for evaluating the heat transfer characteristics and investigating the natural convection effect under different physical conditions. Furthermore, it is of significant importance to study flow and heat transfer characteristics of MFs with varying skeleton structures and porosities [27-29]. For example, copper foam heat exchangers have been utilited in the core flow fields of heat exchanger tubes to effectively improve power generation efficiency of thermoelectric generators by enhancing overall heat transfer capacity [28]. In order to analyze the flow characteristics inside the metal foam, Hu J. H. [29] et al. developed three equivalent alternative models for pressure drop and flow numerical simulations and compared them with the experimental data of copper foam. The pressure prediction accuracy of the honeycomb equivalent model with 20 PPI was obtained to be higher than the other models, with an overall average error of only 4.27%. Experimental results revealed that the outlet velocity displays a negative correlation with porosity on both sides of the MF, and a positive correlation with inlet velocity. Shen H. M. [30] et al. proposed a radiator filled with metal foam and used numerical studies to design models of different shapes such as tetrahedral decahedron, triangular prism and equivalent tetrahedron to analyze the thermal performance of homogeneous metal foam radiator and graded metal foam radiator. It is found that the combined heat transfer performance (CHTP) can be improved by PPI graded metal foam in any direction along the x-axis and y-axis. The solid-liquid phase transition of a copper coconut oil latent heat thermal energy storage (LHTES) unit was simulated by the finite element method for the effect

of anisotropic foam metal on the thermal energy storage of phase change materials by Mehdi G. et al [31]. And localized properties were designed in the vertical direction. The results show that the LHTES unit with anisotropic angle of copper foam saves about 15% (tilting angle of -45°) and 20% (tilting angle of 0°) of charging time. In addition, the melting heat transfer of phase change materials embedded in heterogeneous foam metals is under investigation. It is obtained that the heterogeneous angle shortens the melting time by 24% when the heterogeneous parameter is 0.2. And the charging time of the heterogeneous foam metal is shortened by 11% compared with the normal foam metal [32]. Fully electromagnetic hydrodynamic flow and heat transfer of Casson nanofluid Fe_3O_4-Blood in multiphase media is discussed by Jelena D. Petrović et al. In the channel, an increase in the velocity and temperature of the nanofluid enhances the absolute values of the external power factor and Hartmann number. In addition, increasing the pore factor, Brinkman number and volume fraction increases the temperature of the nanofluid in the channel [33].

Currently, scholars used simulations to predict the thermal performance and photothermal conversion of porous media and metal foam absorbers [34-37]. The distinction is made between the blending of copper foam and other phase change materials to achieve the enhancement of the thermal storage properties of phase change materials at low and medium temperatures. In this experimental study, the experimental study of utilizing metal foam absorbers with different pore densities for photothermal conversion is insufficient, and the thermal efficiency of the absorber needs to be further improved. Therefore, we propose a novel copper foam bulk absorber to improve the thermal efficiency. Specifically, the absorber extends the flow trajectory of the working fluid and achieves a more adequate preheating effect on the air in the absorber channel. In addition, a comparative analysis was conducted between the copper foam absorber and a cavity absorber with pore densities of 10, 20, and 30 PPI (pores per inch), respectively. This work is an experimental validation of previous model predictions and thermal radiation characterization studies of copper foam. The results demonstrate a significant correlation between the photothermal efficiency of the absorber and the pore density of the MF. Notably, the performance of the unit volume absorber shows an increasing trend with higher pore density. These results contribute to the ongoing efforts of the scientific community in developing more effective and efficient heat transfer systems.

2.Construction of the experimental platform

In this study, the specular reflection principle of the disk concentrator is utilized to reflect the sunlight to the focal point of the paraboloid, and then a new designed cavity heat absorber is assembled at the height from the focal point of the disk concentrator. Combined with air compressor, gas flow meter, piping, temperature data logger and other auxiliary equipment, a complete light and heat conversion system is formed. The inner cavity of the absorber can be filled with copper foam with different pore densities as the carrier of heat radiation, and combined with the high-temperature radiation collected by the disk-type concentrator to complete the process of radiation heat transfer. Then the two symmetrical inlets at the top of the heat absorber are fed with air at a certain flow rate, and the gas passes through the copper foam in the inner cavity of the heat absorber to form a forced convection heat transfer process, thus realizing the heat transfer of energy.

The boundary conditions of this experiment include the temperature of the object surface and the air inlet temperature. According to the variation of irradiance, the temperature range of the receiving surface of the heat absorber is measured experimentally to be 450~500 ℃. It is assumed that

the temperature of air at the inlet of the heat absorber is equal to the ambient temperature, which is 25 ± 3 ℃. The velocity of the fluid was synergistically controlled by the flow valve of the air compressor and the switch of the gas flow meter, with flow rates of 20, 30, 40, 50, and 60 $L \cdot min^{-1}$, respectively, whereas the effective emissivity of the copper foam material was 0.95, and the reflectivity was 0.05. In the process of radiative heat transfer, the irradiance range of the experiment, as measured with the BSRN3000 radiation monitoring system, was 570~650 $W \cdot m^{-2}$.

2.1 Design of heat absorber

Fig. 1 (a) is the design of a preheated monolithic absorber structure with separate inner and outer shells. The Fig. 1 (b) illustrates the detailed structural dimensions of the detachable heat absorber. The copper foam (10, 20 and 30 PPI) serves as volumetric solar absorber with similar porosity (95%) and size (100 × 10 mm). The microstructures of the three MF variants are depicted in Fig. 1 (c).

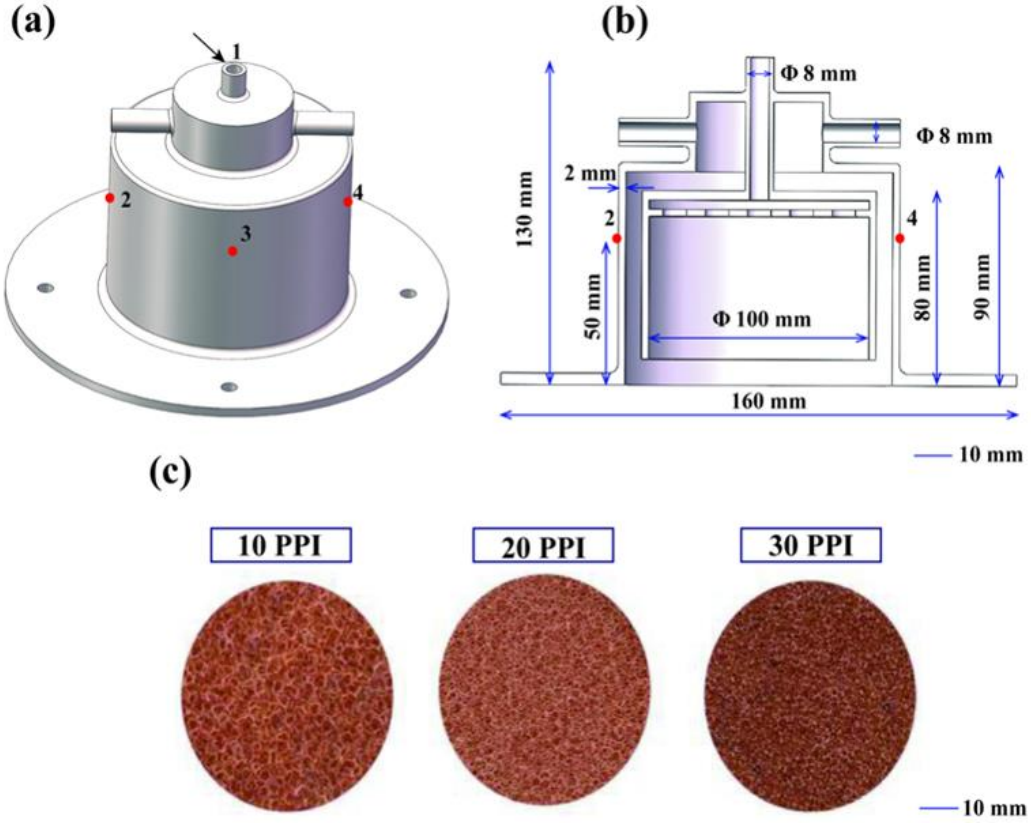

Fig. 1. (a) 3-D structure of volumetric receiver, (b) vertical section marked with the main dimensions, (c) Microstructure of three kinds of metal foam (10, 20, and 30 PPI).

The physical parameters of the air and copper foam materials used during the experiments are shown in Table 1.

Table 1 Physical parameters of working fluid and copper foam

Name	Density ρ/kg·m^{-3}	Specific heat capacity C_p/J/(kg·K)	Thermal conductivity λ/ W·m^{-1}·K^{-1}	porosity
Air (25℃)	1.165	1.005	0.0257	——
Cooper foam	200	100~400	0.2~0.3	95%

2.2 Experimental platform for photothermal conversion

In this work, a two-dimensional manual rotating platform was employed to conduct the photothermal conversion experiment of MF heat absorber (in Fig. 2). The air flow was introduced into the thermal conversion system via a constant pressure air compressor (550 W-8 L). Moreover, the flow rate was measured by a Gas Flowmeter (LZB-10). The working fluid (gas) enters the absorber from the bottom on both sides, and undergoes thermal conversion within the MF section of the absorber. The outlet temperature was measured using a high-temperature resistant GG-K-30 temperature sensor and recorded via a TP700 data recorder.

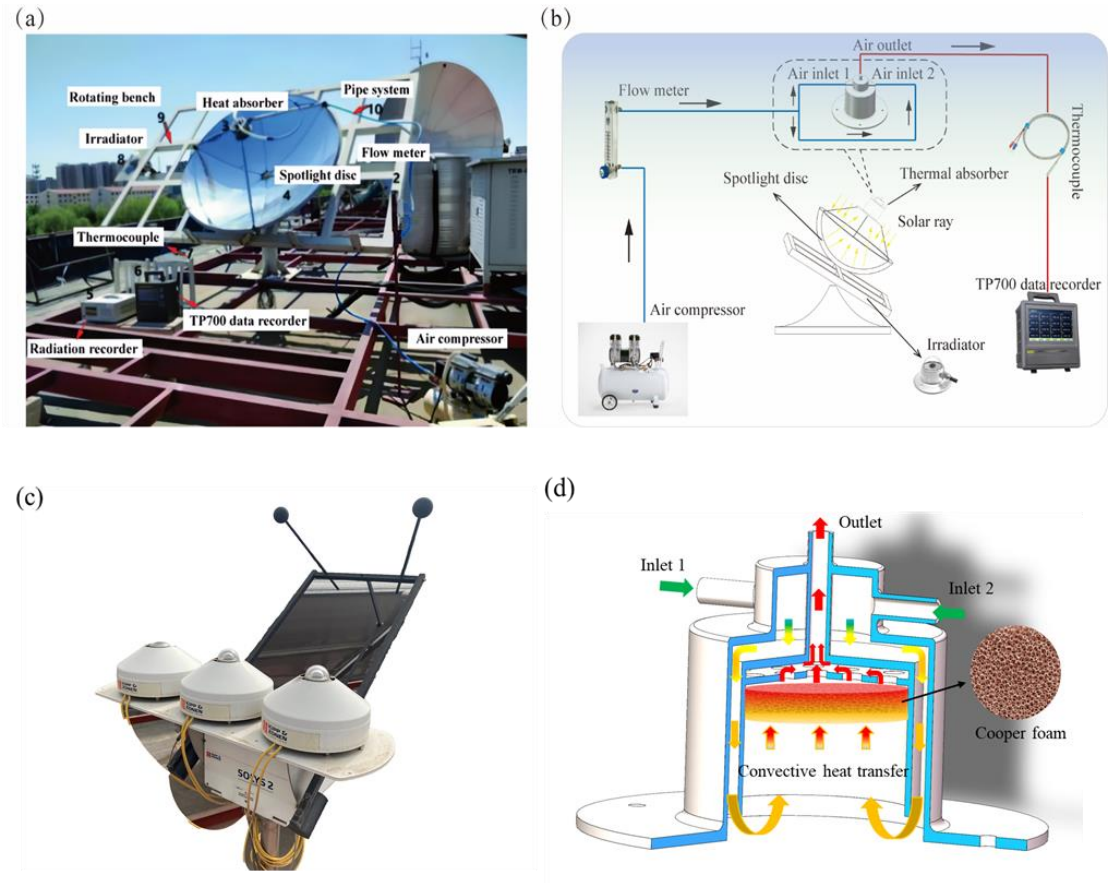

Fig. 2. Platform structure diagram of photothermal conversion experiment (a), schematic (b) of experimental process, BSRN3000 radiation monitoring system (c) and convective heattransfer inside the receiver (d)

2.3 Measuring instruments and errors

The environment was conducted at an ambient temperature of 25 ± 3 ℃, with the air compressor operating at a full-scale flow rate is 60 L·min^{-1} and a working pressure of 0.7 MPa. Airflow rate was measured by an airflow meter with a range of 60 L·min^{-1} and an accuracy of 1.5 L·min^{-1}, while temperature was monitored using a GG-K-30 temperature sensor (The accuracy is ± 0.1 ℃). In addition, the BSRN3000 radiation monitoring system measured the irradiance with an accuracy of 5 W·m^{-2}. The concentrator's reflective efficiency was 0.92. Rotational alignment of the two-dimensional platform was manually adjusted based on sun position. The parameters of the experimental procedure are shown in Table 2.

Table 2 Parameters in the experiment

Ambient temperature	Working pressure of the air compressor	Rated power of air compressor	Air flow rate range	GG-K-30 Temperature Sensor Accuracy	BSRN3000 Radiation Monitoring System Accuracy	Radiation Response Time
25 ± 3 ℃	0.7MPa	550W	20~60 L·min^{-1}	±0.1 ℃	5W·m^{-2}	5s

To ensure reliable and accurate results, the following measurement methods have been used as part of the extraction procedures.

1. All experimental procedures were repeated three times, and the resulting data were presented as the mean value of the four experiments, with errors represented by the standard deviation. The mean value was calculated by dividing the sum of the values by the number of values.

2. The laboratory ambient temperature is approximately 30 °C, and the humidity is approximately 20%.

3. It is assumed that porous foams with different porosity and PPI are homogeneous and isotropic.

4. It is assumed that the device possesses excellent sealing during the experiment.

During the experimental procedures, the maximum error for the temperature data logger was recorded at 0.5 ℃, with the lowest measured temperature T_{min}, being 181.36 ℃. The gas flowmeter's error was determined by relative error, with a measurement range from 10 to 60 L·min^{-1} and an accuracy of ± 2.5%. Given that the minimum flow rate Q_{min} measured during the experiments was 20L·min^{-1}, the maximum relative error can be calculated accordingly. The uncertainty of the data obtained is assessed using the standard deviation, as outlined in equations (1, 2, 3 and 4):

$$\varepsilon_T = \frac{t}{T_{min}} = \frac{0.5}{181.36} = 0.276\% \tag{1}$$

$$\varepsilon_f = \frac{q}{Q_{min}} = \frac{1.5}{20} \times 100\% = 7.5\% \tag{2}$$

$$\varepsilon_{max} = \varepsilon_T + \varepsilon_f = 7.776\% \tag{3}$$

$$\delta=\sqrt{\frac{1}{4}\sum_{i=1}^{4}(x_i-\bar{x})} \tag{4}$$

Where ε_T represents the temperature error, ε_f represents the flow rate error, ε_{max} represents the maximum error of the experimental system, δ represents the standard deviation, x_i and $\bar{x}$ represent the experimental test values and the mean value, respectively.

3. Analysis of experimental results

3.1 Collector Thermal efficiency

To investigate the heat transfer performance of MFs, four groups including heat-absorbing bodies (copper foam with 10, 20, and 30 PPI) and a control group (free-porous metal absorber) were applied to above volumetric receiver in this work. The experimental tests were performed in August 2022 in Hohhot (40.82°N latitude, 111.65°E longitude), Inner Mongolia. All tests were conducted at the time between 12:00 to 15:00. Moreover, for obtaining the steady-state fluid conditions, the pressure regulating pump and flow meter were used to stabilize flow. The outlet temperature of the working fluid from the different heat absorbers were recorded at various levels of irradiances and flow rates. The variation of outlet temperature with irradiance and flow rate is presented in Fig. (3).

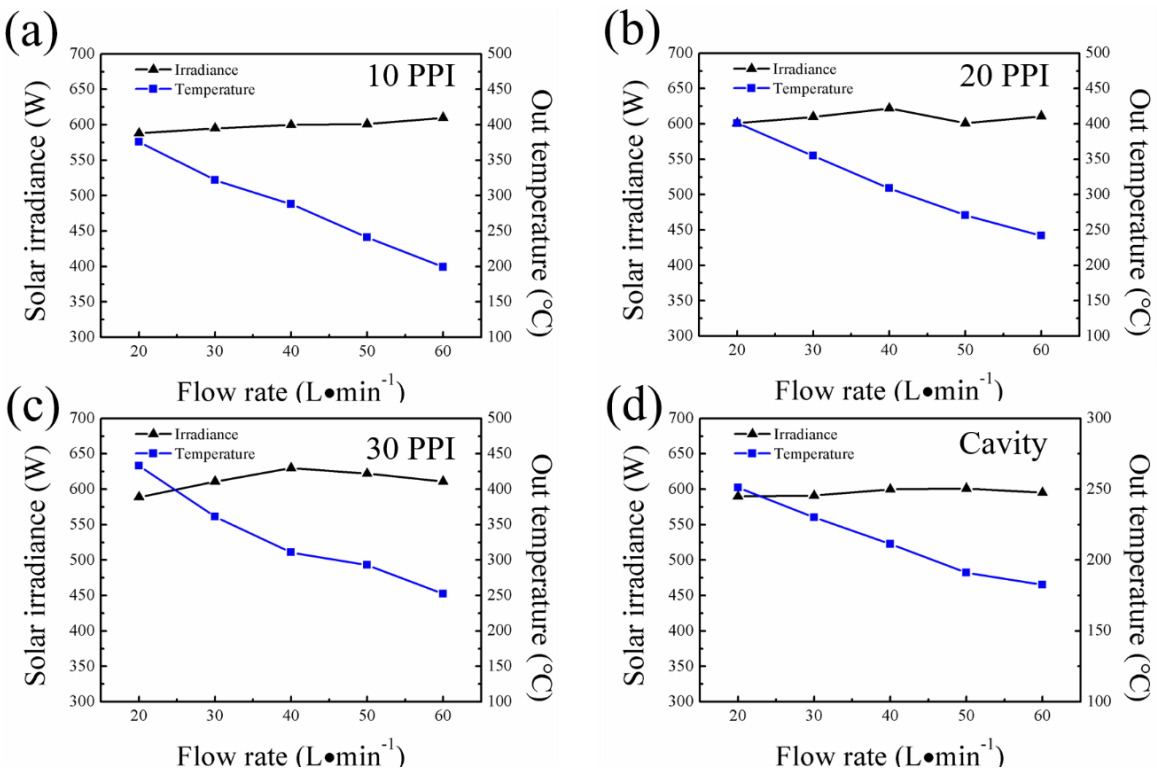

Fig. 3. Variation of outlet temperature with the working medium (gas) flow rate and solar irradiance. (a) 10 PPI copper foam, (b) 20 PPI copper foam, (c) 30 PPI copper foam, and (d) Cavity control group

In this work, the effect of different configurations of copper foams on the temperature difference and the thermal efficiency of disc collector at different flow rates (20~60 L·min^{-1}) was examined. Fig. 3 (a-d) depicted the results of the difference of the inlet and outlet temperatures in

absorber alongside the solar irradiance normal to the aperture. It is indicated that the temperature difference is 433.2 ℃ at 20 L·min^{-1}, which is 180.7 ℃ higher than 60 L·min^{-1} at 30 PPI. According to convective heat transfer theory, the airflow through the porous medium material corresponds to external flow of fluid under turbulent conditions. The calculation of the average heat transfer coefficient of the material's surface is based on the formula $Nu_f = 0.35(s_1/s_2)^{0.2} Re_f^{0.6} Pr^{0.36} (Pr_f/Pr_w)^{0.25}, s_1/s_2 \le 2, (10^3 \le Re \le 2\times10^5)$; $h = Nu \cdot \lambda / d$, where *Nu* denotes the Nusselt number; s_1/s_2 denotes the ratio of transverse to longitudinal pore spacing; *Pr* denotes the Prandtl number; the subscripts *f* and *w* denote the fluid and solid wall surfaces, respectively, and *h* denotes the surface heat transfer coefficient, [W·m^{-2}·K^{-1}]; λ denotes the fluid thermal conductivity, [W·m^{-1}·K^{-1}]; and *d* refers to the material pore size, mm. In addition, the increase in air velocity leads to an increase in the surface heat transfer coefficient of the foam copper's fin structure. It can be determined from tables that the thermal conductivity of foam copper is inversely proportional to its own temperature. The increased air flow with increasing flow rate carries away more heat energy trapped in the foam copper structure, thus leading to a gradual decrease in temperature difference. The temperature difference is gradually increased by increasing of copper foam porosity. This is because foam copper with higher porosity has smaller fin diameters, which increases the material's heat transfer coefficient. Under the same conditions, it is found that the temperature difference ΔT_0: 30 PPI > 20 PPI > 10 PPI. The results showed that the temperature difference of the 30 PPI sample increased by 1.73 times compared to the control group at 20 L·min^{-1}, demonstrating that the porous copper metal can tremendously improve the photothermal conversion capability and enhance the temperature difference.

As represented in Fig. (4), the average outer wall temperatures of four groups were measured by thermal sensors at four monitoring points. The results demonstrated a decrease in wall temperature with an increase in flow rate. However, there were no significant differences of the wall temperature in porous MF groups (with an engineering error within 10%.). Moreover, the wall temperature of the absorber with porous MF is 1.2 to 1.4 times lower than that of the control group at the same working flow. More radiant energy is absorbed by the copper foam material because the internal structure of the molecules and atoms of the copper foam material has a higher frequency vibration compared to the steel material. This results in the thermal conductivity of the copper foam material being much higher than that of the steel material. Additionally, the copper foam has a larger specific surface area than the steel material of the heat absorber shell, thus allowing it to absorb more radiant heat energy. This implies that energy losses can be minimized by using copper foam as a heat-absorbing body.

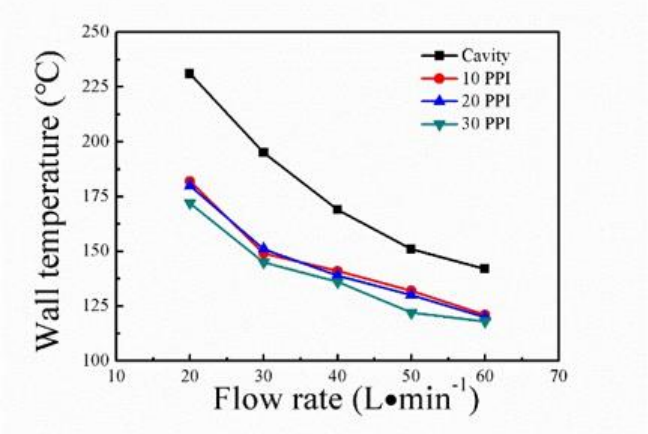

Fig. 4. Relationship between mass flow rate and wall temperature

3.2 Temperature increase at the outlet of heat absorber per unit incident power

During the experiment, the irradiance changed with time and weather conditions, resulting in the instability of outlet temperature and incident power of the system, which was not conducive to the analysis of the experimental data and the description of the phenomena. The direct comparison of the outlet temperatures of the metal foam heat absorbers with three different porosities in Fig. (3) in Section 3.1 is not clear. To address this problem, this work proposes a method for integrating the temperature difference between the inlet and outlet with the incident power (termed: the increase in outlet temperature of the cavity per unit incident power). This parameter is applied to describe the heat transfer enhancement performance of the metal foam heat-absorbing body. The equations of the temperature growth of unit incident power can be written as follows in equations (5, 6 and 7):

$$\zeta = \frac{\Delta T_0}{P_{in}} \tag{5}$$

$$P_{in} = W \square A \tag{6}$$

$$\Delta T_o = T_o - T_e \tag{7}$$

wherein, ΔT_o is the temperature difference between the inlet and outlet, ℃; Where W is the direct irradiance, $W \cdot m^{-2}$; A is the vertical projection area of the reflector disc, m^2.

The average value of ζ is obtained in the flow range under four distinct working conditions after removing the gross error (Fig. 5). It is found that the value of ζ is exclusively depended on the flow rate of the working fluid, exhibiting a diminishing trend with rising fluid flow rates. Notably, the absorbers equipped with internal heat absorbers demonstrated a higher ζ as compared to the cavity configuration, highlighting the significant role of heat-absorbing bodies in enhancing both heat transfer capacity and outlet temperature. The change of ζ is relatively smooth when the working medium (gas) flow rate is between 40 to 50 $L \cdot min^{-1}$. In addition, the temperature of the heat absorber filled with three types of MF decreased, exhibiting the most significant range under 10 PPI as the flow rate exceeded 50 $L \cdot min^{-1}$, with a decrease of 0.172. At 30 and 20 PPI, the temperature decreased by 0.136 and 0.132, respectively. An increase in flow rate causes the absorber to conduct more heat per unit of time, but the increase in the outlet temperature of the absorber per unit of incident power decreases, and the outlet temperature decreases. The higher the flow rate, the more pronounced this phenomenon is. Under identical flow rates, the enhanced heat transfer effect of copper foam heat absorbing materials with different pore densities in the heat transfer process is 30 PPI > 20 PPI > 10 PPI, among which the copper foam with 30 PPI exhibited the most prominent strengthening effect during the heat transfer process. This means that for the same volume, the copper foam material has the most ribbed structures, which maximize the convective heat transfer between the fluid and the material. The high thermal conductivity of the copper foam enables it to absorb and transfer more thermal energy. Therefore, the structural parameters of the copper foam are the main influencing factors for this process. When no heat-absorbing body is present within the cavity, the ζ value exhibited the most substantial decrease when the flow rate exceeded 50 $L \cdot min^{-1}$, decreasing by 0.053. Thus, it can be observed that the flow-node moves backward in the absence of an absorber, and the

decrease is less significant than that when a metal foam heat-absorbing body is incorporated.

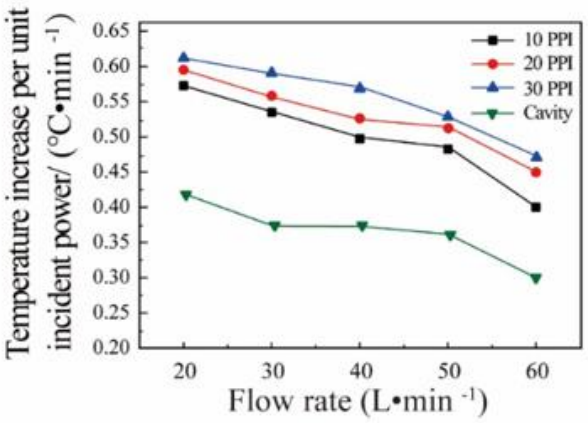

Fig. 5. Relationship between temperature growth and flow of unit incident power

3.3 Comparison of working efficiency of various heat absorbers

The primary objective of heat absorber design is to achieve high photothermal conversion efficiency, which also serves as the primary evaluation criterion. In this work, we comprehensively evaluated the thermal efficiency of this design through experimental analysis. The average thermal efficiency of the three metal foam heat absorbers is illustrated in Fig. (6). Based on the experimental results, it can be concluded that the incorporation of metal foam heat-absorbing bodies within the inner cavity significantly enhances the photothermal conversion efficiency of the heat absorber compared to the cavity alone. The photothermal conversion efficiency of the heat absorber is markedly improved due to the presence of MF (as shown in Fig. 6). The system exhibits a maximum instantaneous efficiency up to 92%, and the highest average efficiency is observed at a porosity of 30 PPI and flow rate of 60 L·min^{-1}, with an accuracy of 87.61%. Under identical flow rates, the thermal efficiency ranking of the heat absorber is observed as follows: 30 PPI > 20 PPI > 10 PPI > Cavity.

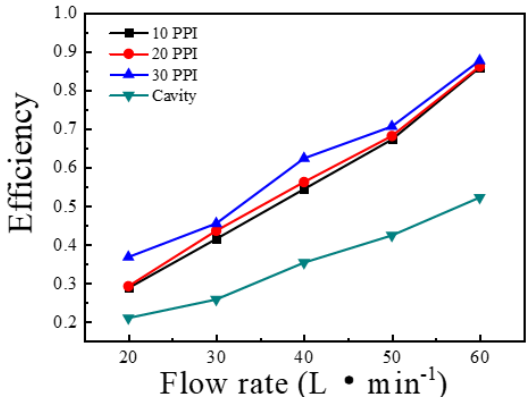

Fig. 6. Average thermal efficiency of three metal foam absorbers

3.4 Heat transfer growth index per unit volume

The incorporation of a heat-absorbing body significantly enhances thermal efficiency. By comparing the thermal conversion efficiency of heat absorbers with and without the presence of the

heat-absorbing body, the result indicate a significant relationship between the structure of the heat-absorbing body and its growth efficiency. In this work, the growth characteristics of the thermal efficiency of metal foam heat-absorbing bodies were also investigated by quantifying the heat transfer enhancement of the MF per unit volume (heat transfer growth index, ψ). The increased heat transfer efficiency per unit volume of MF was utilized to characterize the enhanced heat transfer effect of the copper foam within the absorber. This proposed heat transfer growth index can be employed to predict the overall increase in efficiency after incorporating MF with the same porosity. The formula is expressed as follows in equation (8) of the study:

$$\psi = \frac{\eta_{o-a} - \eta_c}{V} = \frac{C_p m(\Delta T_{o-a} - \Delta T_c)}{WA \cdot V} \tag{8}$$

Where η_{o-a} is the average efficiency of the copper foam and η_c is the average efficiency of the cavity; C_p is the specific heat capacity of air, J/(kg·K); m is the mass flow rate of air, g/s. V is the is the volume of the heat-absorbing body, m^3. ΔT_{o-a} and ΔT_c are the temperature differences between the inlet and outlet of the copper foam and the cavity absorber, respectively. The variation between the average efficiency and the average efficiency of the cavity under the same flow rate is taken and compared with the volume of the respective heat-absorbing bodies.

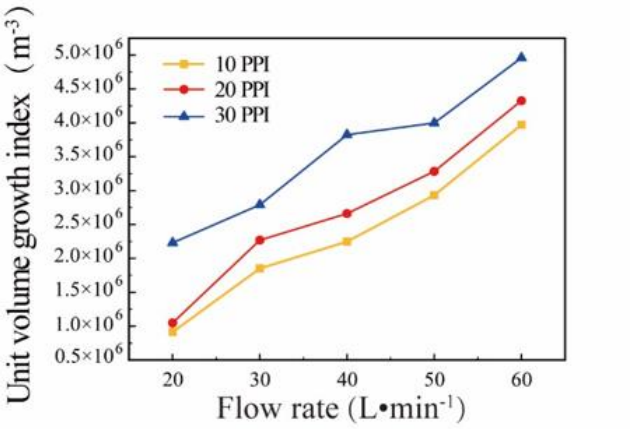

Fig. 7. Heat transfer growth index per unit volume of metal foam under three pore density conditions

Fig. (7) illustrates the relationship between flow rate and the growth index per unit volume for three different MFs. The heat transfer growth index per unit volume increases with increasing air flow rate (Fig. 7). Moreover, the indexes are higher for metals with higher pore densities, especially for the case of 30 PPI, followed by 20 PPI and finally 10 PPI. This is because the higher pore density of the copper foam material results in a larger specific surface area and higher heat transfer efficiency. Larger air flow rates transport more fluid molecules through the copper foam pore structure within the same time period. The fluid flow through the copper foam with a larger specific surface area (30 PPI) further increases the area for convective heat transfer, and the thermal conductivity of the fluid molecules transfers the heat. This leads to a more significant increase in the heat transfer efficiency of the absorber, resulting in a significant increase in absorber efficiency. It can be seen from the figure that the growth patterns of the three types of porosity MFs are the same in the flow rate range of 50 to

60 L·min^{-1}, with the fastest growth rate observed in this range.

Furthermore, Fig. (8) shows the comparison between the thermal efficiencies of absorbers with and without MF. In the work of Jamal-Abad et al. [11], the porous material had 90% porosity with a 30 PPI pore density. In our current work, the porous material has 95% porosity with the same 30 PPI pore density. The results indicate that our work achieves higher thermal efficiency compared to that of Jamal-Abad and M. Valizade [10, 11], owing to the rational absorber structure and the MF at 20~60 L·min^{-1}. Additionally, all the results showed that the thermal efficiency of the absorber with MF increased with the increasing flow.

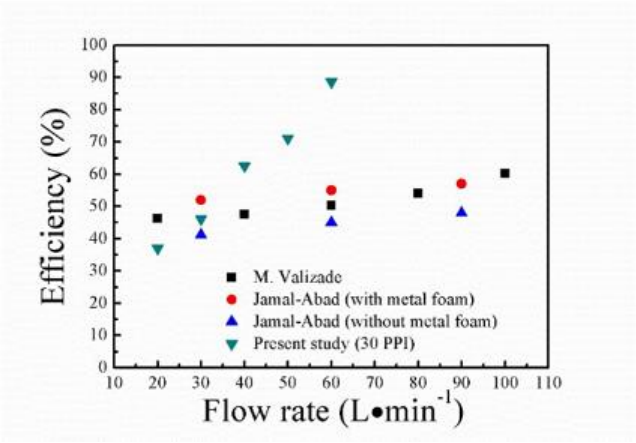

Fig. 8. Comparison of thermal efficiencies of heat absorbers with and without MF

4.Conclusion

In this work, a novel type of heat absorber was designed to strengthen the heat transfer efficiency. Three kinds of copper foam structures with 10, 20, 30 PPI were exploited to investigate the characteristics of the heat exchanger (power, efficiency, flow rate, outlet temperature etc.). All the experimental study of photothermal conversion was carried out on the existing experimental platform. The conclusions are summarized as follows:

(1) The photothermal efficiency of the heat-absorbing body increases gradually with the increasing pore density of the MF as well as working fluid flow rate. Notably, the average photothermal conversion efficiency of the absorber reaches the highest at 30 PPI and a flow rate of 60 L·min^{-1}, reaching 87.61%.

(2) The parameter ζ, defined as the increase in outlet temperature per unit incident power, is proposed to evaluate the heat absorber's performance under varying incident power levels.Moreover, it was found that ζ is closely related to the structure of the heat-absorbing body, and its value generally decreases with increasing flow rate at a constant flow rate.

(3) In this study, a heat transfer enhancement index Ψ per unit volume is formulated to analyze the relationship between the heat-absorbing body's efficiency and its structures. Specifically, the results revealed that the heat transfer enhancement capacity of the heat-absorbing body per unit volume increases with the increase in pore density.

Acknowledgment

The authors wish to acknowledge the support to this work by NSFC funding project (No. 52166016).

Nomenclature

Symbols

A	Area, [m^2]
m	Mass flow rate of air, [g/s]
P_{in}	Unit incident power, [W]
ΔT_o	Temperature difference (inlet and outlet of absorber), [℃]
$\Delta T_{o\text{-}a}$	Temperature differences between the inlet and outlet of the copper foam absorber, [℃]
ΔT_c	Temperature differences between the inlet and outlet of the cavity absorber, [℃]
V	Volume of the heat-absorbing body, [m^3]
W	Direct irradiance, [$W \cdot m^{-2}$]

Shortcuts

MFs	Metal foams
SiC	Silicon carbide
MPA	Metamaterial perfect absorber
PTC	Parabolic trough collector
APDR	Alternative porous disc receiver
PPI	Pores per inch

Greek symbols

ζ	Temperature increase of unit incident power, [W]
ε_T	Temperature error, [%]
ε_f	Flow rate error, [%]
ε_{max}	The maximum error of the experimental system, [%]
δ	Standard deviation
Ψ	Unit volume efficiency growth rate, [%]
$\eta_{o\text{-}a}$	Average efficiency of the cooper metal foam, [%]
η_c	Average efficiency of the cavity, [%]

Reference

[1] Soliman, M. S., *et al.*, Supervisory energy management of a hybrid battery/PV/tidal/wind sources integrated in DC-microgrid energy storage system, *Energy Rep.*, *7*(2021), pp.7728-7740, DOI:10.1016/j.egyr.2021.11.056

[2] Hu T., *et al.*, Photothermal conversion potential of full-band solar spectrum based on beam splitting technology in concentrated solar thermal utilization, *Energy*, *268*(2023), DOI:10.1016/j.energy.2023.126763

[3] Pioro, I., *et al.*, Pros and Cons of Commercial Reactor Designs: Part 2—Current Status and Future Trends in the World Nuclear-Power Industry and Technical Considerations of Nuclear-Power Reactors, in: *Encyclopedia of Nuclear Energy* (Ed. Ehud Greenspan), Elsevier., Amsterdam,

Netherlands, 2021, pp. 288-303
[4] Ali, H. M., Phase change materials based thermal energy storage for solar energy systems, *J. Build. Eng.*, *56*(2022), DOI:10.1016/j.jobe.2022.104731
[5] Liu H., *et al.*, Microencapsulating n-docosane phase change material into CaCO3/Fe3O4 composites for high-efficient utilization of solar photothermal energy, *Renew. Energy*, *179*(2021), pp.47-64, DOI:10.1016/j.renene.2021.07.024
[6] Cui H. Z., *et al.*, Enhancing the heat transfer and photothermal conversion of salt hydrate phase change material for efficient solar energy utilization, *J. Energy Storage*, *49*(2022), DOI:10.1016/j.est.2022.104130
[7] Zhang H. Y., *et al.*, 3D porous copper foam-based shape-stabilized composite phase change materials for high photothermal conversion, thermal conductivity and storage, *Renew. Energy*, *175* (2021), pp. 307-317, DOI:10.1016/j.renene.2021.05.019
[8] Xu S. D., *et al.*, Performance optimization analysis of solar thermophotovoltaic energy conversion systems, *Sol. Energy*, *149*(2017), pp. 44-53, DOI:10.1016/j.solener.2017.03.076
[9] Horikawa, M., *et al.*, Metamaterial perfect absorber-enhanced plasmonic photo-thermoelectric conversion, *Appl. Phys. Express*, *13*(2020), 8, DOI:10.35848/1882-0786/aba56d
[10] Valizade, M., *et al.*, Experimental study of the thermal behavior of direct absorption parabolic trough collector by applying copper metal foam as volumetric solar absorption, *Renew. Energy*, *145*(2020), pp. 261-269, DOI:10.1016/j.renene.2019.05.112
[11] Jamal-Abad, M. T., *et al.*, Heat transfer in concentrated solar air-heaters filled with a porous medium with radiation effects: A perturbation solution, *Renew. Energy*, *91*(2016), pp. 147-154, DOI:10.1016/j.renene.2016.01.050
[12] Xu S., *et al.*, Performance optimization analysis of solar thermophotovoltaic energy conversion systems, *Sol. Energy*, *149*(2017), pp. 44-53, DOI:10.1016/j.solener.2017.03.076
[13] Dong X. H., Research on high temperature heat transfer characteristics of a porous volumetric solar receiver, M.A. thesis, Harbin Engineering University, Harbin, PRC, 2015
[14] Mey-Cloutier, S., *et al.*, Experimental study of ceramic foams used as high temperature volumetric solar absorber, *Sol. Energy*, *136*(2016), pp. 226-235, DOI:10.1016/j.solener.2016.06.066
[15] Reddy, K. S., *et al.*, Experimental investigation of porous disc enhanced receiver for solar parabolic trough collector, *Renew. Energy*, *77*(2015), pp. 308-319, DOI:10.1016/j.renene.2014.12.016
[16] Meng X. L., *et al.*, A vector based free form approach for reflecting concentrator of solar energy, *Sol. Energy*, *153*(2017), pp. 691-699, DOI:10.1016/j.solener.2017.05.070
[17] Yan J., *et al.*, Study on the optical properties of solar dish/triangular cavity receiving system with uniform energy flow distribution, *Journal of Solar Energy*, *41*(2020), 7, pp. 203-213, DOI:10.19912/j.0254-0096.2020.07.030
[18] Yu C. L., Research on heat transfer characteristics of porous media receiver, M.A. thesis, Harbin Engineering University, Harbin, PRC, 2012
[19] Jiang Z. W., Design and experimental study of metal foam solar air heat absorber, M.A. thesis, University of Chinese Academy of Sciences, Beijing, PRC, 2016
[20] Xu C., *et al.*, Numerical investigation on porous media heat transfer in a solar tower receiver, *Renew. Energy*, *36*(2011), 3, pp. 1138-1144, DOI:10.1016/j.renene.2010.09.017
[21] Wang Y. Q., Research on heat transfer characteristics of solar porous medium air receiver, M.A.

Harbin Engineering University, Harbin, PRC, 2015
[22] Ghosh, et al., An experimental study on open cell metal foam as extended heat transfer surface, *Exp. Therm. Fluid Sci., 77*(2016), pp. 28-37, DOI:10.1016/j.expthermflusci.2016.04.010
[23] Cao Y., *et al.,* Heat transfer and thermodynamic analysis of individual and simultaneous effects of revolution, microporous media, magnetic inductor, and nanoparticles in concentrating solar collectors, *Int. Commun. Heat Mass Transfer, 129*(2021), DOI:10.1016/j.icheatmasstransfer.2021.105687
[24] Yang B., *et al.*, Effect of nanoparticles and metal foams on heat transfer properties of PCMs, *Int. Commun. Heat Mass Transfer, 179*(2022), DOI:10.1016/j.ijthermalsci.2022.107567
[25] Wang Z. L, *et al.*, Effect of copper metal foam proportion on heat transfer enhancement in the melting process of phase change materials, *Appl. Therm. Eng., 201*(2022), DOI:10.1016/j.applthermaleng.2021.117778
[26] Tian Y. *et al.*, A numerical investigation of heat transfer in phase change materials (PCMs) embedded in porous metals, *Energy, 36*(2011), 9, pp. 5539-5546, DOI:10.1016/j.energy.2011.07.019
[27] Yang T. H, *et al.*, Numerical study of flow and heat transfer in a three-dimensional metal foam considering different direction micropores in skeleton structure, *Int. Commun. Heat Mass Transfer, 134*(2022), DOI:10.1016/j.icheatmasstransfer.2022.106052
[28] Li Y. Z, *et al.*, Influence of foamed metal core flow heat transfer enhancement on the performance of thermoelectric generators with different power generation characteristics, *Therm. Sci. Eng. Prog., 31*(2022), DOI:10.1016/j.tsep.2022.101300
[29] Hu J. H., *et al.*, Experiment and simulation investigation of flow characters in metal foam, *Numer. Heat Transfer B, 83*(2022), 1-2, pp. 24-38, DOI:10.1080/10407790.2022.2105124
[30] Shen H. M., *et al.*, Pore-scale numerical investigation on comprehensive heat transfer performance of homogeneous and graded metal foam heat sinks based on tetrakaidecahedron cell, *Therm. Sci., 00*(2023), pp. 237-237
[31] Ghalambaz M., *et al.*, Anisotropic metal foam design for improved latent heat thermal energy storage in a tilted enclosure, *Int. J. Mech. Sci., 238*(2023), DOI:10.1016/j.ijmecsci.2022.107830
[32] Ghalambaz M., *et al.*, Mathematical modeling of heterogeneous metal foams for phase-change heat transfer enhancement of latent heat thermal energy storage units, *Appl. Math. Model., 115*(2023), pp. 398-413, DOI:10.1016/j.apm.2022.10.018
[33] Petrovic J. D., *et al.*, Electromagnetic hydrodynamic flow and heat transfer of a casson nanofluid Fe3O4-Blood in a porous medium, *Therm. Sci., 27*(2023), 6A, pp. 4461-4472
[34] Wei G. S., *et al.*, Experimental study on the radiative properties of open-cell porous ceramics, *Sol. Energy, 149*(2017), pp. 13-19, DOI:10.1016/j.solener.2017.04.002
[35] Randrianalisoa J., *et al.*, Thermal conductive and radiative properties of solid foams: Traditional and recent advanced modelling approaches, *C. R. Phys., 15*(2014), 8-9, pp. 683-695, DOI:10.1016/j.crhy.2014.09.002
[36] Marri G K., *et al*., Experimental and numerical investigations on the effect of porosity and PPI gradients of metal foams on the thermal performance of a composite phase change material heat sink, *Int. Commun. Heat Mass Transfer, 164*(2021), DOI:10.1016/j.ijheatmasstransfer.2020.120454
[37] Kuruneru S T W, *et al*., Application of porous metal foam heat exchangers and the implications of particulate fouling for energy-intensive industries, *Chem. Eng. Sci., 228*(2020),

DOI:10.1016/j.ces.2020.115968

RECEIVED DATE: 30.10.2023.
DATE OF CORRECTED PAPER: 16.12.2023.
DATE OF ACCEPTED PAPER: 14.03.2024.